Available online at www.sciencedirect.com

ScienceDirect

Procedia Structural Integrity 24 (2019) 390–397

Structural Integrity Procedia

www.elsevier.com/locate/procedia

AIAS 2019 International Conference on Stress Analysis

Piezoresistive dynamic simulations of FDM 3D-Printed embedded strain sensors: a new modal approach

Marco Maurizi[a,*], Filippo Cianetti[b], Janko Slavič[c], Guido Zucca[d], Massimiliano Palmieri[b]

[a]NTNU - Norwegian University of Science and Technology –Department of Mechanical Engineering, 7491 Trondheim, Norway
[b]University of Perugia - Department of Engineering, Via G. Duranti 93, 06125 Perugia, Italy
[c]Faculty of Mechanical Engineering, University of Ljubljana, Aškerčeva 6, 1000 Ljubljana, Slovenia
[d]Aeronautica Militare, Centro Sperimentale di Volo, Dipartimento di Tecnologia dei Materiali per l'Aeronautica e lo Spazio, Aeroporto Militare M. De Bernardi, Via Pratica di Mare, 0000040, Pomezia (RM), Italy

Abstract

3D-printing of embedded piezoresistive sensors has been making the numerical dynamic simulation necessary to develop new smart 3D structures, which have essentially a dynamic nature. This work researches the potentiality of coupled piezoresistive finite-element modeling (FEM) to dynamically simulate 3D-printed embedded sensors. A new modal approach is proposed, proving theoretically the linearity of the weak coupled-field model, under the assumption of constant current and small perturbations. This method has been numerically validated comparing it to the nonlinear full-transient analysis both in the time and frequency domain, providing a reduction factor of the computation time of ∼ 600. Finally, the piezoresistive model has been experimentally validated, highlighting its real effectiveness. The computation time performances of the proposed linear approach are opening new possibilities to dynamically simulate whatever piezoresistive smart structure in the preliminary design phase.

Keywords: Piezoresistive Simulations; Additive Manufacturing; Embedded Sensors; Finite Element Modeling; Dynamic Simulations; Fused Deposition Modeling; Smart Structures

1. Introduction

Numerical simulations of sensors have become fundamental in the recent years due to the development of 3D-printed embedded sensors O'Donnell et al. (2014), that require to be designed concurrently with the structure in which they are integrated. The great enhancement of the fused deposition modeling (FDM) 3D-printing technique Muth et al. (2014); Leigh et al. (2012) and the novel functional materials Wang et al. (2017); Nadgorny and Ameli (2018), which has made possible to print sensors (functional materials) and structures (non-sensing materials) in the same build

* Corresponding author. Tel.: +39-327-780-3296.
E-mail address: marcomaurizi06@gmail.com

10.1016/j.prostr.2020.02.036

cycle Maurizi et al. (2019), realizing 3D-printed Smart Structures O'Donnell et al. (2014), has required to rethink the product design, especially the preliminary phase of numerical simulations. Among the 3D-printed integrated sensors, the piezoresistive strain sensory elements have been the object of a significant research interest Muth et al. (2014). The need to simulate the entire piezoresistive sensors' behavior, both electrical and structural, has therefore been growing with the ability of the Additive Manufacturing to co-print sensors and structures, making possible to realize free-shaped embedded sensors Dijkshoorn et al. (2018). In the preliminary phase of the product design, a numerical coupled-field simulation is necessary to optimize the sensors' shape, dimensions and location inside the structure, forecasting the sensors' sensitivity variation by a numerical parametric sensitivity analysis, without spending time and resources in experimental tests. Coupled-field analyses are already performed to simulate classical strain gauges Thangamani et al. (2008); however, the birth of the 3D-printing embedded sensing have been making this kind of simulation essential to completely design 3D-printed Smart Structures Gooding and Fields (2017). The only structural numerical modeling is just in itself an unavoidable, but not sufficient, instrument to design embedded sensors, giving the opportunity to estimate in advance the interaction between structure and sensor. Indeed, structural problems, such as stress discontinuities and slippage in the boundaries between sensor and component, could occur, generating critical zones in which the fatigue phenomenon could produce failure; therefore, using the structural finite-element modeling allows to identify these problems and adopt engineering solutions to avoid or reduce them. The inherent dynamic Smart Structures' behavior Vepa (2010) has made inescapable the necessity to simulate them dynamically, especially for the integrated strain sensors. Indeed, dynamic strain measurements are essential in many applications, such as medical diagnostics Sharafeldin et al. (2018), 3D-printed aerospace components Wang et al. (2017) and fatigue life monitoring in smart structures Stark et al. (2014). Despite this, piezoresistive dynamic simulations of 3D-printed smart structures have not been researched. In this work, piezoresistive dynamic simulations of FDM 3D-printed strain sensory elements embedded in structures are performed and validated by experimental measurements carried out in the previous work Maurizi et al. (2019). In particular, a modal (linear) approach for piezoresistive coupled-field dynamic analyses to simulate embedded strain sensors is proposed and numerically and experimentally validated.

2. Theoretical Background

The FDM 3D-printed embedded strain sensory elements used in this work are made of conductive PLA (see Section 4); therefore, the basic constitutive equation, which describes the electrical behavior of the sensor, is the point form of the Ohm's law $\boldsymbol{E} = \boldsymbol{\rho}\,\boldsymbol{J}$ (see Falcon et al. (2014)). Where $\boldsymbol{E}$ is the electric field vector (3×1), $\boldsymbol{\rho}$ is the electric resistivity tensor (3×3) (symmetric) and $\boldsymbol{J}$ is the current density vector (3×1). Considering the quasi-static approximation of the system of Maxwell's equations, it follows that the electric field is irrotational; hence, the relation $\boldsymbol{E} = -\boldsymbol{\nabla} V$ can be obtained, introducing in this way the electric scalar potential V, measured in [Volt]. For a generic continuum conductor, by the previous equations and the continuity equation $\boldsymbol{\nabla} \cdot \boldsymbol{J} = 0$, neglecting the time-variation of V, the following governing equation for the sensor's electrical behavior is obtained:

$$-\boldsymbol{\nabla} \cdot (\boldsymbol{\rho}^{-1}\, \boldsymbol{\nabla} V) = 0 \tag{1}$$

The application of the variational principle, the finite-element discretization to Eq. (1) and the approximation of the voltage over one element through the element shape functions matrix N of size $(n_V^e \times 1)$, where n_V^e is the number of degrees of freedom (DOF) of voltage of one element, gives the element electrical conductivity coefficient matrix of size $(n_V^e \times n_V^e)$, as follows ANSYS Inc. U.S.A. (2009).

$$\boldsymbol{K_e^V} = \int_{vol} (\boldsymbol{\nabla N}^T)^T \boldsymbol{\rho}^{-1}\, \boldsymbol{\nabla N}^T d(vol) \tag{2}$$

Indeed, the finite-element equation for one element that relates the nodal voltage vector V (with an abuse of notation) and the nodal current vector I, of size $(n_V^e \times 1)$, can be written as $\boldsymbol{K_e^V}\, \boldsymbol{V} = \boldsymbol{I}$.

To simulate dynamically the embedded strain sensors a piezoresistive finite-element model has been implemented in this work. The coupled-field finite-element matrix equation for the global system, with an abuse of notation (using $\boldsymbol{V}$ and $\boldsymbol{I}$ for the system), in the time domain is given by ANSYS Inc. U.S.A. (2009):

$$\begin{bmatrix} \boldsymbol{M} & \boldsymbol{0} \\ \boldsymbol{0} & \boldsymbol{0} \end{bmatrix} \begin{Bmatrix} \ddot{\boldsymbol{x}} \\ \ddot{\boldsymbol{V}} \end{Bmatrix} + \begin{bmatrix} \boldsymbol{C} & \boldsymbol{0} \\ \boldsymbol{0} & \boldsymbol{C}^V \end{bmatrix} \begin{Bmatrix} \dot{\boldsymbol{x}} \\ \dot{\boldsymbol{V}} \end{Bmatrix} + \begin{bmatrix} \boldsymbol{K} & \boldsymbol{0} \\ \boldsymbol{0} & \boldsymbol{K}^V \end{bmatrix} \begin{Bmatrix} \boldsymbol{x} \\ \boldsymbol{V} \end{Bmatrix} = \begin{Bmatrix} \boldsymbol{F} \\ \boldsymbol{I} \end{Bmatrix} \tag{3}$$

where, defining n as the number of structural DOF, $\boldsymbol{M}$ is the mass matrix $(n \times n)$, $\boldsymbol{C}$ is the damping matrix $(n \times n)$, $\boldsymbol{K}$ is the stiffness matrix $(n \times n)$, $\boldsymbol{x}$ is the displacement vector $(n \times 1)$ and $\boldsymbol{F}$ is the force vector $(n \times 1)$. The first row of Eq. (3) is the classical structural equation. The second row represents the electrical part of the model, in which $\boldsymbol{C}^V$ is the global dielectric permittivity coefficient matrix $(n_V \times n_V)$, that is neglected in this work; $\boldsymbol{K}^V$ is the global electrical conductivity coefficient matrix $(n_V \times n_V)$. n_V is the number of DOF of voltage of the global electrical system. The numerical problem is weakly coupled ANSYS Inc. U.S.A. (2009). Indeed, $\boldsymbol{\rho}$ is variable with the stress tensor ($\boldsymbol{S}$ is the tensor representation (3×3)), hence, with respect to the structural DOF $\boldsymbol{x}$. Thus, $\boldsymbol{K}^V$ is not constant, depending on $\boldsymbol{x}$. The electric resistivity $\boldsymbol{\rho}$ changes as consequence of applied loads, as follows ANSYS Inc. U.S.A. (2009):

$$\boldsymbol{\rho} = \boldsymbol{\rho}^0 (\boldsymbol{I}_d + \boldsymbol{r}) \tag{4}$$

where $\boldsymbol{\rho}^0$ is the resistivity matrix (3×3) of the unloaded material, $\boldsymbol{I}_d$ is the identity matrix (3×3) and $\boldsymbol{r}$ is the relative change in resistivity (3×3), whose vector representation $\widetilde{\boldsymbol{r}}$ (6×1) is given by ANSYS Inc. U.S.A. (2009):

$$\widetilde{\boldsymbol{r}} = \boldsymbol{\pi} \widetilde{\boldsymbol{S}} \tag{5}$$

in which $\boldsymbol{\pi}$ represents the piezoresistive stress matrix (6×6), while $\widetilde{\boldsymbol{S}}$ is the vector representation (6×1) of the stress tensor $\boldsymbol{S}$. The component π_{ij} of the matrix $\boldsymbol{pi}$ is a scalar value, which relates the i-th component of the relative change of resistivity vector $\Delta\boldsymbol{\rho}/\boldsymbol{\rho}$ (6×1) to the j-th component of the stress vector $\boldsymbol{S}$.
Considering only the first row of Eq. (3), it can be solved, under the hypothesis of mechanical linearity, by the well-known modal approach Cianetti et al. (2017). Additionally, using the state space representation of the reduced modal system (modal state space), whatever $\boldsymbol{P}$ structural quantity can be obtained both in the time and frequency domain. In particular, $\boldsymbol{P}(t)$ results in:

$$\boldsymbol{P}(t) = \boldsymbol{\Phi}_P^T \boldsymbol{q}(t) \tag{6}$$

where $\boldsymbol{\Phi}_P$ is the matrix $(m \times r)$ of the structural quantity mode shapes, considering m modes and r outputs, and $\boldsymbol{q}(t)$ is the vector $(m \times 1)$ of the modal coordinates.
The FRF matrix $\boldsymbol{H}_{PF}$ force-to-physical quantity of size $(r \times p)$ can be computed as follows:

$$\boldsymbol{H}_{PF} = \boldsymbol{\Phi}_P^T \boldsymbol{H}_q(f) \tag{7}$$

where $\boldsymbol{H}_q(f)$ is the FRF matrix force-to-modal coordinates of size $(m \times p)$, obtained by the modal state space Kranjc et al. (2016).

3. Proposed Modal Approach

Software for numerical simulations based on finite-element modeling, such as Ansys Mechanical APDL (Ansys, Inc.) used in this work, implement piezoresistive coupled-field analysis solving Eq. (3) by a nonlinear solver (e.g. Newton-Raphson) because the matrix $\boldsymbol{K}^V$ depends on $\boldsymbol{x}$, that is a DOF of the system. To overcome the nonlinear setting of the problem, represented by Eq. (3), the authors proposes a linear modal approach.
Based on the consideration that the system of Eq. (3) is weakly coupled, the two equations can be solved separately; in particular, the structural equation has to be solved before the electrical part, which needs the structural solution to be solved (see Section 2). The problem is reduced to find out the solution of the electrical part (neglecting the contribution of the matrix $\boldsymbol{C}^V$), knowing the structural solution, that is the nodal displacements $\boldsymbol{x}(t)$ and every mechanical quantity, such as the stress tensor $\boldsymbol{S}$ on the elements' centroid.
To simulate the discrete electric circuit represented by the FDM 3D-printed embedded piezoresistive sensor, it is possible to assume that the nodal current vector $\boldsymbol{I}(t) = \boldsymbol{k}$, with $\boldsymbol{k} = \boldsymbol{const}.\ \forall\, t$, in the nodes where the current is applied (zero elsewhere). In this way, a resistance (the sensory element) powered by constant current is obtained (see Fig. 3 in Section 5).
In the time domain, the sensor's electrical response on one node (the mode shapes have dimensions $(m \times 1)$) results in:

$$\Delta V(t)/V_0 = \boldsymbol{\Phi}^T_{\Delta V/V_0}\, \boldsymbol{q}(t) \tag{8}$$

where $\boldsymbol{\Phi}^T_{\Delta V/V_0}$ is the matrix $(m \times 1)$ of the relative change of voltage, assumed to be the electrical sensor's response. The proposed modal approach has been implemented as reported in the scheme in Fig. 1.

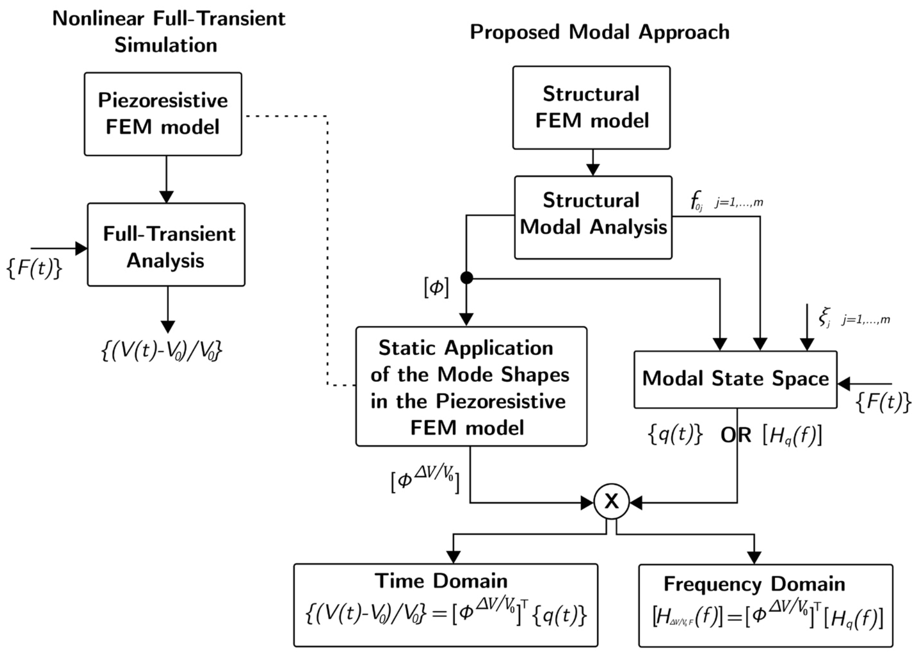

Fig. 1. Implementation schemes of the nonlinear full-transient analysis and the proposed linear (modal) approach.

4. Test Case

In the previous work Maurizi et al. (2019) the abilities of FDM 3D-printed piezoresistive sensors embedded in structures to perform dynamic measurements and identify the system's natural frequencies have been proven; besides, the nonlinearities, the temperature effects, the dynamic range and the frequency range of the 3D-printed embedded sensors have been investigated.
This work starts from the quasi-static and dynamic measurements performed in Maurizi et al. (2019), using the 3D-printed embedded strain sensor as test case, and testing the effectiveness and the performances of the proposed modal approach numerically and experimentally. The embedded strain sensory element and the structure have been printed in the same build cycle by using a FDM printer dual extruder (Ultimaker 3), as shown in Fig. 2a.

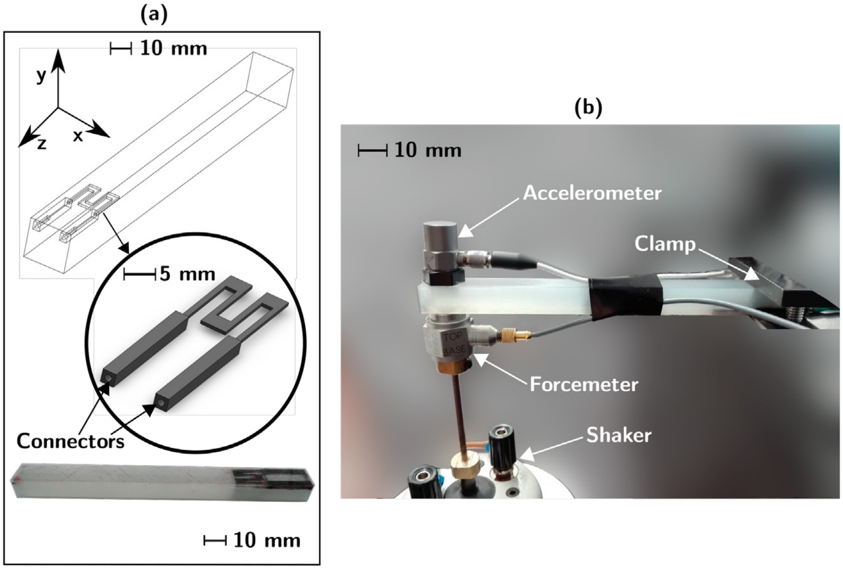

Fig. 2. Sample and its experimental configuration. **(a)** CAD model of the sample and the embedded sensor and the 3D-printed manufactured specimen. **(b)** Cantilever beam experimental set-up.

5. Piezoresistive Dynamic Simulations

In the previous research activity Maurizi et al. (2019) the experimentation has played a central role to investigate the 3D-printed embedded strain sensor's dynamic capabilities. However, in a preliminary design phase of the product the experimental tests should be avoided to reduce the time and the costs.
Therefore, starting from the experimental results of Maurizi et al. (2019), piezoresistive coupled-field numerical dynamic simulations have been performed, implementing the approach described in Section 3.
To perform piezoresistive simulations, the elements solid227 have been adopted to mesh the integrated sensor. The electrical boundary conditions for the sensor have been imposed to create an analogy between a simple concentrated parameter model and the FEM model, which represents a continuum model; in Fig. 3 the similarity is shown. A current of intensity $I = 0.2$ mA has been applied to the nodes on the two sensor's surfaces shown in Fig. 3. Additionally, a zero voltage has been imposed to the nodes on one of the two sensor's surfaces as reference voltage.
Considering random ergodic white noise as input force, the numerical validation of the proposed modal approach is shown in Fig. 4, in which the comparison in the time domain between the nonlinear full-transient simulation and the modal approach is carried out. As evident, the match is almost perfect.
In Table 1, the computation time comparison between the full-transient and modal approach is highlighted, showing how the proposed approach is 616 times (in this case) faster than the nonlinear method. Finally, the experimental validation of the numerical piezoresistive model is shown in Fig. 5.

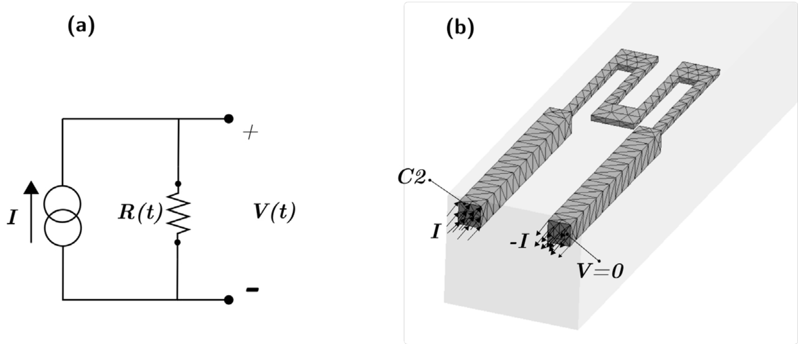

Fig. 3. Analogy between the concentrated parameters model of the sensor and its FEM model, and relative boundary conditions. **(a)** Concentrated parameters model. **(b)** Finite-element model.

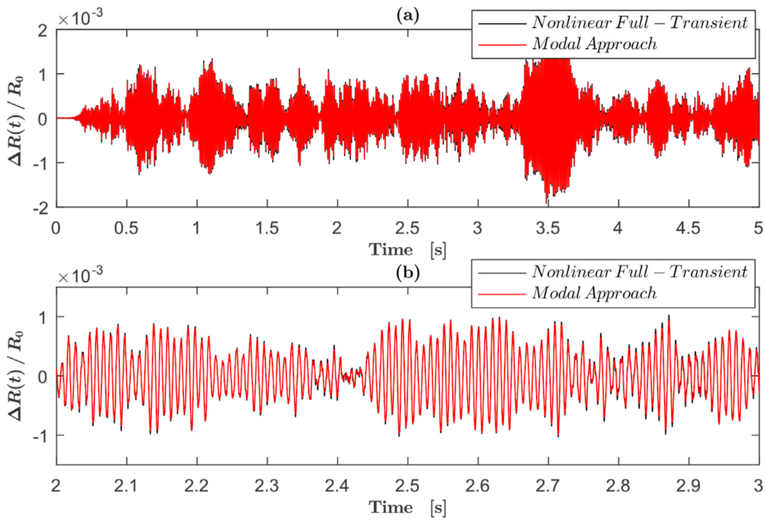

Fig. 4. Comparison between piezoresistive full-transient analysis and modal approach in the time domain with $F(t)$ as input, in the range 5 Hz to 800 Hz. (a) Sensor's response up to $T = 5$ s. (b) Zoom in the range 2 s to 3 s.

Table 1. Computation time comparison full-transient and modal approach.

Simulation Approach	Computation Time [s]
Nonlinear Full-Transient	5.6878512×10^5
Modal Approach	922.23

6. Conclusions

The potentialities of numerical dynamic analyses to simulate FDM 3D-printed embedded strain sensory elements have been researched. The structural simulations have been used to show the capability of numerical analysis to forecast possible structural problems, which can occur in case of 3D-printed sensors embedded in systems. To completely simulate piezoresistive sensory elements, piezoresistive coupled-field analyses have been implemented, proposing a modal (linear) approach, which allows to avoid the nonlinear solver implemented by commercial finite-element software. Besides, it can be assessed that the proposed method has validity under the hypothesis of constant electrical

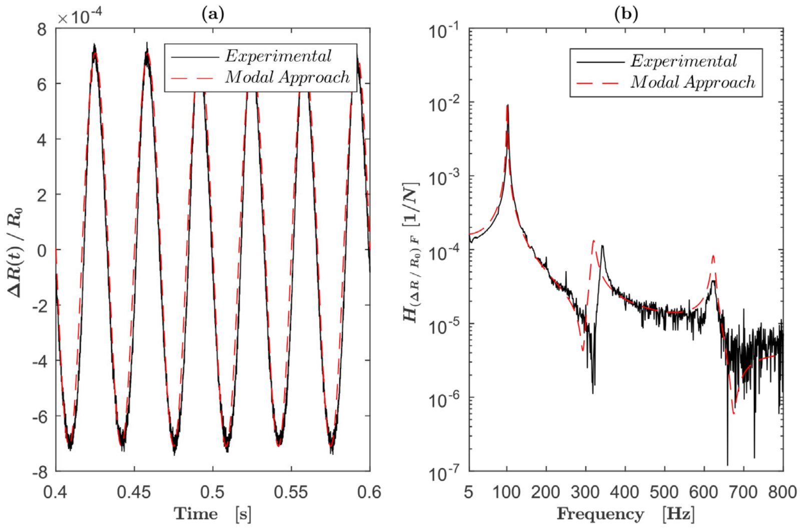

Fig. 5. Validation piezoresistive FEM model with experimental results of Maurizi et al. (2019). **(a)** Quasi-static conditions at 30 Hz in the time domain, zoom in the range 0.4 s to 0.6 s. (b) Dynamic conditions in the frequency domain, in the range 5 Hz to 800 Hz.

current boundary conditions, while the hypotheses on the matrix $\boldsymbol{\pi}$ are not limiting. The computation time's reduction of this method, which has been numerically and experimentally validated, is considerably high (more than 600 times in this work), if compared to the complete nonlinear approach. Additionally, despite the uncertainty of the numerical model to represent perfectly a real 3D-printed embedded sensor, due to the presence of sources of noise in the reality, the proposed linear approach represents a powerful and fast method to predict numerically the sensor's response and its sensitivity (gauge factor) in advance compared to the experimental tests.

This work shows the abilities of numerical piezoresistive models to simulate and completely characterize the 3D-printed embedded strain sensor's behavior, highlighting how the proposed modal approach is able to strongly reduce the computation time.

References

ANSYS Inc. U.S.A., 2009. Theory Reference for the Mechanical APDL and Mechanical Applications. Knowledge Creation Diffusion Utilization 3304, 724–746.

Cianetti, F., Palmieri, M., Slavič, J., Braccesi, C., Morettini, G., 2017. The effort of the dynamic simulation on the fatigue damage evaluation of flexible mechanical systems loaded by non-gaussian and non stationary loads. International Journal of Fatigue 103, 60 – 72. URL: http://www.sciencedirect.com/science/article/pii/S0142112317302347, doi:https://doi.org/10.1016/j.ijfatigue.2017.05.020.

Dijkshoorn, A., Werkman, P., Welleweerd, M., Wolterink, G., Eijking, B., Delamare, J., Sanders, R., Krijnen, G.J., 2018. Embedded sensing: integrating sensors in 3-d printed structures. Journal of Sensors and Sensor Systems 7, 169.

Falcon, N., Falcon, O., Robledo, F., 2014. Causal generalization of the ohm's law in transient phenomena quasi-static. International Journal of Engineering Science and Innovative Technology (IJESIT) 3, 315–322.

Gooding, J., Fields, T., 2017. 3d printed strain gauge geometry and orientation for embedded sensing, in: 58th AIAA/ASCE/AHS/ASC Structures, Structural Dynamics, and Materials Conference, p. 0350.

Kranjc, T., Slavič, J., Boltežar, M., 2016. A comparison of strain and classic experimental modal analysis. JVC/Journal of Vibration and Control 22, 371–381. doi:10.1177/1077546314533137.

Leigh, S.J., Bradley, R.J., Purssell, C.P., Billson, D.R., Hutchins, D.A., 2012. A Simple, Low-Cost Conductive Composite Material for 3D Printing of Electronic Sensors. PLoS ONE 7, 1–6. doi:10.1371/journal.pone.0049365.

Maurizi, M., Slavič, J., Cianetti, F., Jerman, M., Valentinčič, J., Lebar, A., Boltežar, M., 2019. Dynamic Measurements Using FDM 3D-Printed Embedded Strain Sensors. Sensors 19, 2661. URL: https://www.mdpi.com/1424-8220/19/12/2661, doi:10.3390/s19122661.

Muth, J.T., Vogt, D.M., Truby, R.L., Mengüç, Y., Kolesky, D.B., Wood, R.J., Lewis, J.A., 2014. Embedded 3D printing of strain sensors within highly stretchable elastomers. Advanced Materials 26, 6307–6312. doi:10.1002/adma.201400334, arXiv:NIHMS150003.

Nadgorny, M., Ameli, A., 2018. Functional Polymers and Nanocomposites for 3D Printing of Smart Structures and Devices. ACS Applied Materials & Interfaces 10, 17489–17507. doi:10.1021/acsami.8b01786.

O'Donnell, J., Ahmadkhanlou, F., Yoon, H.S., Washington, G., 2014. All-printed smart structures: a viable option?, in: Active and Passive Smart Structures and Integrated Systems 2014, International Society for Optics and Photonics. p. 905729.

Sharafeldin, M., Jones, A., Rusling, J., 2018. 3d-printed biosensor arrays for medical diagnostics. Micromachines 9, 394.

Stark, B., Stevenson, B., Stow-Parker, K., Chen, Y., 2014. Embedded sensors for the health monitoring of 3d printed unmanned aerial systems, in: 2014 International Conference on Unmanned Aircraft Systems (ICUAS), IEEE. pp. 175–180.

Thangamani, U., Yunus, H.M., Chekima, A., 2008. Design and simulation of force sensor with piezoresistive rectangular strain gauge. Journal - The Institution of Engineers, Malaysia 69, 38–44.

Vepa, R., 2010. Dynamics of smart structures. John Wiley & Sons.

Wang, X., Jiang, M., Zhou, Z., Gou, J., Hui, D., 2017. 3D printing of polymer matrix composites: A review and prospective. Composites Part B: Engineering 110, 442–458. URL: http://dx.doi.org/10.1016/j.compositesb.2016.11.034, doi:10.1016/j.compositesb.2016.11.034.